

Optimal Partitioning of Non-Convex Environments for Minimum Turn Coverage Planning

Megnath Ramesh, Frank Imeson, Baris Fidan, and Stephen L. Smith

Abstract—In this paper, we tackle the problem of generating a turn-minimizing coverage plan for a robot operating in an indoor environment. In coverage planning, the number of turns in the generated path affects the time to cover the environment and the quality of coverage, e.g. tools like cameras and cleaning attachments commonly have poor performance around turns. In many existing turn-minimizing coverage methods, the environment is partitioned into the least number of *ranks*, which are non-intersecting rectangles of width equal to the robot’s tool width. This partitioning problem is typically solved using heuristics that do not guarantee optimality. In this work, we propose a linear programming (LP) approach to partition the environment into the least number of axis-parallel (horizontal and vertical) ranks with the goal of minimizing the number of turns taken by the robot. We prove that our LP method solves this problem optimally and in polynomial time. We then generate coverage plans for a set of indoor environments using the proposed LP method and compare the results against that of a state-of-the-art coverage approach.

I. INTRODUCTION

Coverage path planning is an automation challenge in which a robot carrying a sensing or a coverage tool is required to traverse a path such that the tool covers all points of the environment [1]. This problem has many applications, including cleaning [2], agriculture [3], model reconstruction [4] and inspection of 3D structures [5]–[7]. Recently, coverage planning has also found applications in the autonomous disinfection of hospitals during the COVID-19 pandemic [8]. An ideal coverage plan covers all feasible regions with the tool in the shortest time. However, this is an NP-Hard problem [9] and hence is generally simplified into multiple sub-problems. One simplification is to partition the environment into regions that are each covered individually by the tool and to then plan a tour of the regions. The partitioning sub-problem can be formulated to generate a high-quality coverage path by optimizing for a set of metrics.

The quality of a coverage path can be measured in terms of a variety of factors; notably the time taken to complete a coverage plan, the area covered and the number of turns taken by the robot. In this paper, we aim to generate a high-quality coverage path by minimizing the turns taken by the robot. The reasoning behind this choice is two-fold: (i) the robot travels slower around turns, and (ii) the coverage

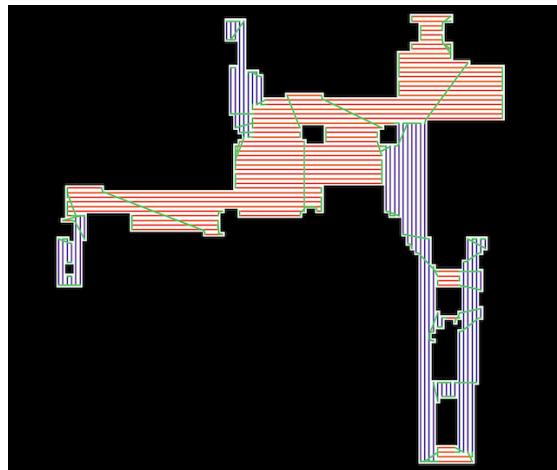


Fig. 1: Coverage Plan of an indoor environment generated using the proposed LP method.

quality often degrades when turning. For instance, a cleaning tool cannot pick up water and dust properly while turning.

A. Related Work

Boustrophedon decomposition [10] is a widely known approach in robotic coverage planning. In this approach, the environment is partitioned into *cells* (usually convex). The cells are individually covered in a back-and-forth sweeping pattern along parallel straight-line paths. There are also turn-minimizing variations of this approach where each cell is covered along an optimal orientation that minimizes the number of angular transitions during coverage. The number of angular transitions in the coverage path approximates the number of turns. The cell’s orientation is obtained using different criteria; by studying the geometry of each cell [11] or its convex hull [12], or minimizing a cost function that models the robot’s turns [13]. These variations work well to incorporate multiple coverage directions for minimizing turns. However, the partitioning step can also be time-intensive for complex real-world environments. Additionally, while these approaches aim to minimize the number of angular transitions to cover each cell, they do not guarantee minimization of the total number of angular transitions. In this paper, we address these shortcomings by creating a partition of the environment that minimizes the total number of angular transitions without incorporating Boustrophedon decomposition. We also guarantee that our proposed method solves this partitioning problem optimally.

Another category of approaches, referred to as *grid-based approaches*, is to approximate the environment as a union of

M. Ramesh (m5ramesh@uwaterloo.ca) and S. L. Smith (stephen.smith@uwaterloo.ca) are with the Department of Electrical and Computer Engineering and B. Fidan (fidan@uwaterloo.ca) is with the Department of Mechanical and Mechatronics Engineering, at the University of Waterloo, Waterloo ON, Canada

F. Imeson (frank.imeson@avidbots.com) is with Avidbots Corp., Waterloo ON, Canada

uniform *grid cells* where the robot must cover all accessible grid cells. Our proposed approach falls under this category. The shape of the grid cells is usually a square [14] but there are approaches that use regular hexagons [15]. Coverage planning for a grid approximation can be solved by generating a spanning-tree of the grid cells [16], [17]. This approach attempts to minimize the length of the coverage plan within the grid approximation. Recently, learning-based coverage planning methods that use grid representations of the environment have also been introduced [18]–[21]. These approaches however do not aim to minimize the number of turns, while our proposed method does.

Minimizing turns to cover a grid approximation is proven to be an NP-Hard problem [22]. The problem can be simplified by restricting the robot’s motion during coverage to only horizontal and vertical motions. This restriction follows the predominantly rectilinear nature of real-world indoor environments. Vandermeulen et. al. proposed an approach that solves this simplified problem using a heuristic to further partition the grid approximation into the minimum number of horizontal and vertical rectangles [23]. These rectangles are as wide as the coverage tool and are referred to as *ranks*. The idea behind this approach is to reduce the total number of angular transitions while covering the environment along the ranks. The heuristic-based method runs iteratively and performs well with a large number of iterations. However, heuristic-based methods are not guaranteed to reach the optimal solution for the problem, whereas our method solves this problem optimally.

B. Contributions

In this paper, we propose a Linear Programming (LP) formulation to partition a grid approximation of an environment into the least number of axis-parallel (horizontal and vertical) ranks. We first formulate the partitioning problem as a Mixed Integer Linear Program (MILP) (Section III). We then prove that the LP obtained by relaxing the constraints of the MILP is guaranteed to provide an optimal solution to the problem in polynomial time (Section IV). The generated ranks are then connected to obtain the full coverage plan by formulating the connection problem as a Generalized Travelling Salesman Problem (GTSP) (Section V). We then present our simulation results on a set of test environments (Section VI) and compare the performance of our algorithm with a state-of-the-art heuristic-based coverage approach [23].

II. PROBLEM DEFINITION AND SOLUTION APPROACH

A. Coverage Planning Problem

Consider a closed and bounded set $\mathcal{W} \subseteq \mathbb{R}^2$ representing our indoor environment. Let \mathcal{O} denote the set of obstacles or inaccessible points of the environment. Let $\widetilde{\mathcal{W}} = \mathcal{W} \setminus \mathcal{O}$ specify the accessible points of the environment.

With this representation of the environment, the goal of the coverage problem is to plan a path so that the tool covers all accessible areas in the given environment. The tool has a footprint $\mathcal{A}(\omega) \subset \mathbb{R}^2$ relative to the robot’s position $\omega \in \mathbb{R}^2$. Conventionally, $\mathcal{A}(\omega)$ is represented by a simple geometric

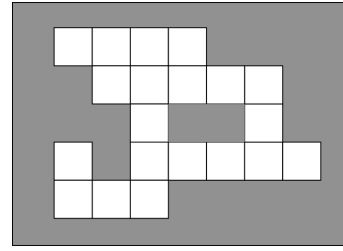


Fig. 2: An Integral Orthogonal Polygon with light squares representing the polygon and grey areas representing the boundaries and holes.

shape such as a square of a fixed width $l > 0$ centered at ω [1], [16], [22], [23]. For this work, we adopt a square coverage tool of width l .

The tool may not be able to cover the environment entirely as there will likely be coverage gaps near the boundaries. Let $\widehat{\mathcal{W}} \subseteq \widetilde{\mathcal{W}}$ be the points of the environment that can be covered by the tool. The goal of the coverage problem is then to plan a path such that the union of the coverage tool footprint when swept along the path is equal to $\widehat{\mathcal{W}}$. An extension of this problem is to optimize the plan such that it minimizes a predefined cost function.

B. Solution Approach: Decomposition

In this paper, we approach the coverage problem by partitioning the environment into non-intersecting regions that are each covered individually. We then compute a tour of the regions using a GTSP formulation and generate our full coverage plan. The typical objective of the tour is to minimize the transition time between the regions.

C. IOP and Minimum Rank Partitioning Problem

We now consider a decomposition that can help quantify the number of potential turns in the coverage plan. We therefore look at decomposing the environment into regions that will each be covered with a straight-line path (no turns). A *rank* is the cumulative footprint of the coverage tool when traversing a straight-line path. For a square coverage tool of width l , a rank is a rectangular region of width l .

Let us now consider a set of orthogonal axes in the plane of the environment and look at a simplified coverage problem where our square tool can move only in axis-parallel directions during coverage (horizontal and vertical). For this simplified coverage problem, we obtain a grid-based approximation of $\widetilde{\mathcal{W}}$ that can be partitioned into non-intersecting horizontal and vertical ranks. We refer to this approximation as an Integral Orthogonal Polygon (IOP), viz. a union of square grid cells of size $l \times l$ that approximates the environment [22].

We now make some assumptions to ensure our IOP can be partitioned into axis-parallel ranks. Since the square coverage tool can fully occupy a grid cell, we assume that the robot starts the coverage plan at the center of a grid cell and traverses through the IOP by moving from one grid cell to another. We also assume that all paths of the robot have endpoints at the center of the IOP grid cells, which is similar

auxiliary variable y_h^i that bounds $\text{end}_H(c_i)$. The upper index (i) of y_h^i matches the lower index of c_i . We also introduce a set of binary variables to denote whether a cell is horizontally or vertically oriented. For the horizontal case, we introduce x_h^i which equals 1 if $\text{orient}(c_i) = H$ and 0 otherwise. For the left neighbour, $c_l = \text{left}(c_i)$, we observe the following:

$$x_h^i - x_h^l = \begin{cases} 1 & \text{if } \text{orient}(c_i) = H \text{ and} \\ & \text{orient}(\text{left}(c_i)) = V \\ 1 & \text{if } \text{orient}(c_i) = H \text{ and } \text{left}(c_i) \text{ is} \\ & \text{a border identifier} \\ -1 & \text{if } \text{orient}(c_i) = V \text{ and} \\ & \text{orient}(\text{left}(c_i)) = H \\ 0 & \text{otherwise} \end{cases}$$

The above, along with a non-negativity constraint, gives an encoding of y_h^i where $y_h^i \geq \text{end}_H(c_i)$.

$$\begin{aligned} y_h^i &\geq x_h^i - x_h^l \\ y_h^i &\geq 0 \end{aligned}$$

With these constraints, we observe that minimizing y_h^i gives us an optimal solution where $y_h^i = \text{end}_H(c_i)$. We now determine the values of y_h^i for all grid cells using the following system of vector inequalities:

$$\mathbf{y}_h \geq A_H \mathbf{x}_h \quad (3)$$

$$\mathbf{y}_h \geq \mathbf{0} \quad (4)$$

where \mathbf{y}_h and \mathbf{x}_h are n -dimensional vectors composed of the variables y_h^i and x_h^i respectively. On further inspection, A_H in (3) is the *node-arc incidence (NAI) matrix* [24] of the directed graph G_H (see Fig. 4) composed of all horizontal path flows for an IOP grid cell from its left neighbour/border identifier. Similarly, we encode $\text{end}_V(c)$ using the auxiliary variable vector \mathbf{y}_v and the NAI matrix A_V of the directed graph G_V (Fig. 4).

Using the defined matrices and vectors, we write the following MILP to solve Problem 1:

$$\min \sum_{i=0}^n y_h^i + \sum_{i=0}^n y_v^i \quad (5)$$

$$\text{s.t. } A_H \mathbf{x}_h - \mathbf{y}_h \leq \mathbf{0} \quad (6)$$

$$A_V \mathbf{x}_v - \mathbf{y}_v \leq \mathbf{0} \quad (7)$$

$$\mathbf{x}_h + \mathbf{x}_v = \mathbf{1} \quad (8)$$

$$\mathbf{x}_h, \mathbf{x}_v \in \{0, 1\}^n \quad \mathbf{y}_h, \mathbf{y}_v \geq \mathbf{0} \quad (9)$$

where $\mathbf{1}$ is the column vector of ones and $\mathbf{0}$ is the vector of zeros. Eq. (8) ensures that each grid cell is assigned one of two orientations (either x_h^i or x_v^i equals 1). The objective in Eq. (5) gives us the number of ranks while \mathbf{x}_h and \mathbf{x}_v gives us the corresponding grid cell orientations. The solution of the MILP gives the minimum rank partition as determined by the grid cell orientations.

From this MILP, we obtain an LP relaxation using Eqs. (5)-(8) by replacing the binary variables \mathbf{x}_h and \mathbf{x}_v in (9) with continuous variables.

$$\mathbf{x}_h, \mathbf{x}_v, \mathbf{y}_h, \mathbf{y}_v \geq \mathbf{0} \quad (10)$$

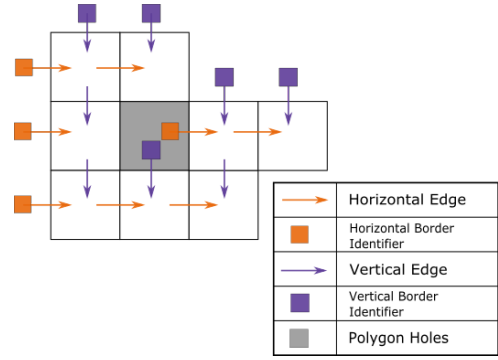


Fig. 4: An illustration of the directed graphs G_H (orange) and G_V (purple) for an IOP.

Proposition 1. *The relaxed LP denoted by Eqs. (5)-(8) and (10) computes an integral optimal solution and hence solves Problem 1 in polynomial time.*

IV. PROOF OF PROPOSITION 1

In general, solving MILPs is NP-hard while LPs can be solved in polynomial time [25]. An LP relaxation of a MILP in general will not yield optimal integral solutions. However, our LP relaxation belongs to a special class of problems that yield integral optimal solutions. This is mainly because of our use of NAI matrices, which are totally unimodular (TU) [26]. A matrix is TU if the determinants of all its square submatrices are in $\{-1, 0, 1\}$ [24], [27]. In this section, we prove that the matrix of all constraints in Eqs. (5)-(8) and (10) is totally unimodular. It will then follow from the Hoffman-Kruskal Principle [28] that the relaxed LP can directly solve the MILP in polynomial time, since our matrix is TU.

Theorem 1 (Hoffman-Kruskal Principle [28]). *If an integral matrix A is TU, then for an integral vector \mathbf{b} , the polyhedron $\{\mathbf{x} \in \mathbb{R}^n \mid A\mathbf{x} \leq \mathbf{b}\}$ has integral coordinates.*

Since the polyhedron has integral coordinates, the resulting optimal solution for the LP defined in the polyhedron is also integral.

Lemma 2. *The constraints of the LP relaxation are totally unimodular.*

Proof. First, we write our problem in Standard Equality Form (SEF) using slack variables to eliminate the inequality constraints. We then remove the summations from the objective function using a vector multiplication with $\mathbf{1}$. The rewritten problem is:

$$\min \quad \mathbf{1}^T \mathbf{y}_h + \mathbf{1}^T \mathbf{y}_v \quad (11)$$

$$\text{s.t. } A_H \mathbf{x}_h - \mathbf{y}_h + \mathbf{z}_h = \mathbf{0} \quad (12)$$

$$A_V \mathbf{x}_v - \mathbf{y}_v + \mathbf{z}_v = \mathbf{0} \quad (13)$$

$$\mathbf{x}_h + \mathbf{x}_v = \mathbf{1} \quad (14)$$

$$\mathbf{x}_h, \mathbf{x}_v, \mathbf{y}_h, \mathbf{y}_v, \mathbf{z}_h, \mathbf{z}_v \geq \mathbf{0} \quad (15)$$

The constraints are now of the form $A\mathbf{x} = \mathbf{b}$:

$$A = \begin{bmatrix} A_H & \bar{\mathbf{0}} & -I & \bar{\mathbf{0}} & I & \bar{\mathbf{0}} \\ \bar{\mathbf{0}} & A_V & \bar{\mathbf{0}} & -I & \bar{\mathbf{0}} & I \\ I & I & \bar{\mathbf{0}} & \bar{\mathbf{0}} & \bar{\mathbf{0}} & \bar{\mathbf{0}} \end{bmatrix} \quad (16)$$

$$\mathbf{b} = [\mathbf{0}^T \quad \mathbf{0}^T \quad \mathbf{1}^T]^T \quad (17)$$

$$\mathbf{x} = [\mathbf{x}_h^T \quad \mathbf{x}_v^T \quad \mathbf{y}_h^T \quad \mathbf{y}_v^T \quad \mathbf{z}_h^T \quad \mathbf{z}_v^T]^T \quad (18)$$

where $\bar{\mathbf{0}}$ is the matrix of zeros and I is the identity matrix. Clearly \mathbf{b} is an integral vector.

To prove A is TU, let us start with the matrix:

$$\tilde{A} = \begin{bmatrix} A_H^T & \bar{\mathbf{0}} & I \\ \bar{\mathbf{0}} & A_V^T & I \end{bmatrix}$$

Each row of the NAI matrices A_H and A_V signifies a directed edge in the graph, with a +1 for the source grid cell (outgoing), a -1 for the sink grid cell (incoming), and 0s otherwise [24].

Due to this construction, \tilde{A} satisfies the following sufficient conditions for TU matrices as outlined in [28] and [27].

- 1) All elements are in $\{-1, 0, +1\}$ (all entries in A_V and A_H are either -1, 0, or +1).
- 2) Each column of \tilde{A} has at most two non-zero elements (each column of A_H^T and A_V^T will have two non-zero entries, one for the source and one for the sink).
- 3) There exists a partition of the rows of \tilde{A} into two disjoint sets T_1 and T_2 such that:
 - If any column of \tilde{A} contains two nonzero entries of the same sign, then one is in a row of T_1 and the other is in a row of T_2 .
 - If any column of \tilde{A} contains two nonzero entries of the opposite sign, then they are both in a row of T_1 or in a row of T_2 .

For our formulation, T_1 consists of all rows in:

$$[A_H^T \quad \bar{\mathbf{0}} \quad I]$$

and T_2 consists of all rows in:

$$[\bar{\mathbf{0}} \quad A_V^T \quad I]$$

It follows from [24] that the transpose of \tilde{A} is also TU. We can construct A from \tilde{A}^T by appending columns of the positive and negative signed unit matrices \bar{I} and $-\bar{I}$ where:

$$\bar{I} = \begin{bmatrix} I & \bar{\mathbf{0}} & \bar{\mathbf{0}} \\ \bar{\mathbf{0}} & I & \bar{\mathbf{0}} \\ \bar{\mathbf{0}} & \bar{\mathbf{0}} & I \end{bmatrix}$$

Appending these columns preserves the total unimodularity of the resulting matrix, see [24]. Because of this, the matrix A is TU, which completes the proof of Lemma 2. \square

Since the constraints are TU, it follows from Theorem 1 and [25] that the relaxed LP computes optimal integral solutions for the formulated MILP in polynomial time. We can therefore solve Problem 1 optimally in polynomial time using the LP.

TABLE I: Robot dynamics used for simulations

Maximum Linear velocity	100 <i>cm/s</i>
Linear Acceleration	50 <i>cm/s²</i>
Angular velocity	30°/s

V. TOUR GENERATION

From the LP formulated in Section III, we merge cells that are covered by the same rank to obtain the rank partition. We then solve Problem 2 to plan our full coverage plan by obtaining a tour of the ranks.

The tour generation is formulated into a Generalized Travelling Salesman Problem (GTSP) which computes a visitation order for the ranks. Using a GTSP formulation offers us the flexibility to use existing approaches and heuristics to compute the tour [29]–[31]. We employ a similar formulation as proposed by Bochkarev et. al. [11]. Each set in the GTSP graph consists of two vertices representing the two directions to traverse a rank. If a rank has endpoints a and b , the rank can either be covered *from a to b* or *from b to a*. The GTSP aims to visit one vertex in each set (a rank traversed in a specific direction) and minimizes the cost of the tour.

The edge costs between the vertices in different sets of the GTSP graph are given by the subsequent time to travel between rank endpoints along an obstacle-free *transition path*. Each transition path is computed by constructing a visibility graph within the IOP boundaries and planning the shortest path using an A* search [32]. The resulting path is a sequence of straight lines and intermediary turns. The travel time is then determined by assuming semi-holonomic robot dynamics where the robot stops to turn in-place with a constant angular velocity. When travelling in a straight line, the robot has constant acceleration/deceleration and can reach a maximum linear velocity.

VI. SIMULATION EXPERIMENTS

In this section, we test our coverage planning approach by running simulations on a variety of indoor environments. We combined robotic scans of real-world indoor environments to generate 4 hybrid maps for our experiments. We then compare the results of our planning approach to that of the coverage planning approach proposed in [23].

A. LP Simulation

To simulate our LP approach, we generate an IOP for each environment and compute the rank partition by orienting the grid cells using Eqs. (5)-(8) and (10). The GTSP formulation in Section V is then used to compute a cost-minimizing tour of the ranks. Table I shows our choice of values to simulate the robot's dynamics and compute the transition costs.

The algorithm was prototyped in Python 3 using GLPK [33] to solve the LP and GLNS [29] to solve the formulated GTSP problem. Fig. 1 shows a coverage plan generated for one of our test maps (Map 2 in results) with the horizontal (orange) and vertical (purple) ranks as determined by the LP solver. The tour transitions between the ranks (green lines) are computed by the GTSP solver. On average, the

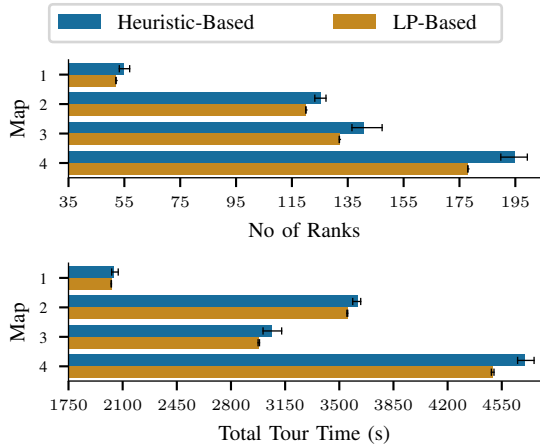


Fig. 5: Results of comparison between LP-method and heuristic-based coverage method [23].

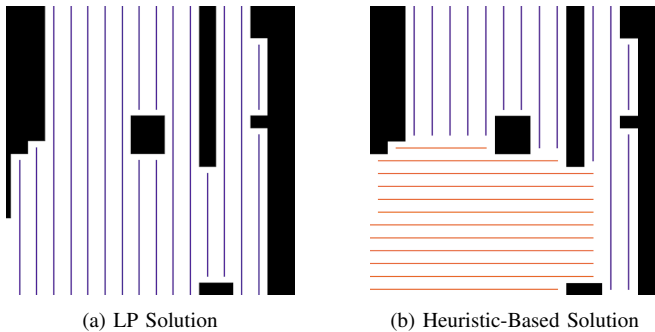


Fig. 6: Comparison of ranks generated in a region.

LP computes the orientations in 0.47 seconds, which makes the problem of computing the ranks almost negligible when compared to the GTSP (12.5 seconds).

B. Comparisons

We also compared our algorithm to the heuristic-based coverage approach proposed in [23]. To solve the same problem of IOP coverage, we only include the interior ranks from the approach and ignore the perimeter ranks. The coverage algorithm in [23] is an iterative algorithm where the performance of the algorithm is linked to the number of iterations it is allowed to run for. To standardize the comparison, we performed two types of experiments: (i) compare the solutions of both approaches when run for the same time (ii) compare the average time for both approaches to reach the optimal solution.

For the first experiment, the heuristic-based approach is run for the same amount of time as the LP. We conducted 10 trials on each of the 4 maps and display the data collected as bar graphs in Fig. 5. The metrics for comparison were: (i) the number of ranks generated by the algorithm, and (ii) total time taken for the coverage tour. Each bar denotes the mean value of the metric, while the whisker (thin I like bar) shows the range of all values obtained in the experiments. We observe that the LP method consistently outperforms the heuristic-based method in all metrics. The LP method returns

TABLE II: Comparison of times to reach optimal number of ranks. Each trial is limited to 30 minutes.

Map	LP-Based Coverage		Heuristic-Based Coverage [23]	
	Optimal # Ranks	Average Runtime (s)	Average time to reach optimal (s)	Best solution achieved
1	52	0.09	0.35	52
2	120	0.47	22.06	120
3	132	0.21	Reached limit	133
4	178	0.61	Reached limit	181

a constant number of ranks for each environment with the number always being less than or equal to that computed using the heuristic-based method. The LP method is also more predictable as the tour time does not deviate much from the mean.

For the second experiment, we compare how long each approach takes to find the optimal number of ranks. We terminate each approach once it reaches the optimal solution and the runtime is recorded. Each run is limited to 30 minutes, after which we record the best solution achieved by the run. The experiment was run for 10 trials on each map, and the results are shown in Table II. We observe that the LP partitions the environment optimally with an average runtime < 1 s. The heuristic-based algorithm is able to reach the optimal solutions for maps 1 and 2, but fails to solve the partitioning problem optimally for maps 3 and 4 within the time limit. The LP solver on average obtains the optimal solution much faster.

We also inspected the best solutions of both algorithms to better understand the differences in solution quality. An interesting case is shown in Figure 6. Here, the LP partitions the region into less ranks than the heuristic-based solution. The heuristic was stuck in a local minima, likely because its orientation assignments are heavily influenced by the partition's shape and neighbours, see [23]. The heuristic could get the optimal if the initial solution is seeded optimally, but that becomes less likely when the environment has many such regions like this.

VII. CONCLUSION

In this paper, we proposed a linear programming (LP) approach to partition an indoor region into thin axis-parallel ranks with the goal of minimizing the number of turns needed to cover the region. We proved that this approach computes the optimal number of ranks in polynomial time. Our simulations verify that the proposed LP approach indeed achieves the minimum number of ranks for a region. Also, the proposed approach has shown to have lower coverage tour times when compared to a heuristic-based algorithm. For future work, it is aimed to leverage the fast performance of the LP to develop an online turn-minimizing coverage planner for uncertain dynamic environments.

ACKNOWLEDGMENT

This work was supported by Canadian Mitacs Accelerate Project IT16435 and Avidbots Corp, Kitchener, ON, Canada.

REFERENCES

- [1] E. Galceran and M. Carreras, "A survey on coverage path planning for robotics," *Robotics and Autonomous Systems*, vol. 61, no. 12, pp. 1258–1276, 2013.
- [2] C. Hofner and G. Schmidt, "Path planning and guidance techniques for an autonomous mobile cleaning robot," *Robotics and Autonomous Systems*, vol. 14, no. 2, pp. 199–212, 1995.
- [3] I. A. Hameed, "Intelligent coverage path planning for agricultural robots and autonomous machines on three-dimensional terrain," *Journal of Intelligent and Robotic Systems: Theory and Applications*, vol. 74, no. 3-4, pp. 965–983, 2014.
- [4] R. Almadhoun, T. Taha, L. Seneviratne, and Y. Zweiri, "A survey on multi-robot coverage path planning for model reconstruction and mapping," *SN Applied Sciences*, vol. 1, no. 8, 2019.
- [5] S. Song, D. Kim, and S. Jo, "Online coverage and inspection planning for 3D modeling," *Autonomous Robots*, vol. 44, no. 8, pp. 1431–1450, 2020.
- [6] W. Jing, D. Deng, Z. Xiao, Y. Liu, and K. Shimada, "Coverage Path Planning using Path Primitive Sampling and Primitive Coverage Graph for Visual Inspection," in *2019 IEEE/RSJ International Conference on Intelligent Robots and Systems (IROS)*, 2019, pp. 1472–1479.
- [7] I. Z. Biundini, M. F. Pinto, A. G. Melo, A. L. M. Marcato, L. M. Honório, and M. J. R. Aguiar, "A Framework for Coverage Path Planning Optimization Based on Point Cloud for Structural Inspection," *Sensors*, vol. 21, no. 2, p. 570, 2021.
- [8] B. Nasirian, M. Mehrandezh, and F. Janabi-Sharifi, "Efficient Coverage Path Planning for Mobile Disinfecting Robots Using Graph-Based Representation of Environment," *Frontiers in Robotics and AI*, vol. 8, p. 4, 2021.
- [9] E. M. Arkin, S. P. Fekete, and J. S. Mitchell, "Approximation algorithms for lawn mowing and milling," *Computational Geometry*, vol. 17, no. 1-2, pp. 25–50, 2000.
- [10] H. Choset and P. Pignon, "Coverage Path Planning: The Boustrophedon Cellular Decomposition," *Field and Service Robotics*, pp. 203–209, 1998.
- [11] S. Bochkarev and S. L. Smith, "On minimizing turns in robot coverage path planning," in *2016 IEEE International Conference on Automation Science and Engineering (CASE)*, 2016, pp. 1237–1242.
- [12] M. Torres, D. A. Pelta, J. L. Verdegay, and J. C. Torres, "Coverage path planning with unmanned aerial vehicles for 3D terrain reconstruction," *Expert Systems with Applications*, vol. 55, pp. 441–451, 2016.
- [13] J. Jin and L. Tang, "Optimal Coverage Path Planning for Arable Farming on 2D Surfaces," *Transactions of the ASABE*, vol. 53, no. 1, pp. 283–295, 2010.
- [14] T. M. Cabreira, P. R. Ferreira, C. D. Franco, and G. C. Buttazzo, "Grid-Based Coverage Path Planning With Minimum Energy Over Irregular-Shaped Areas With UAVs," in *2019 International Conference on Unmanned Aircraft Systems (ICUAS)*, 2019, pp. 758–767.
- [15] X. Kan, H. Teng, and K. Karydis, "Online Exploration and Coverage Planning in Unknown Obstacle-Cluttered Environments," *IEEE Robotics and Automation Letters*, vol. 5, no. 4, pp. 5969–5976, 2020.
- [16] Y. Gabriely and E. Rimon, "Spanning-tree based coverage of continuous areas by a mobile robot," *Annals of Mathematics and Artificial Intelligence*, vol. 31, no. 1-4, pp. 77–98, 2001.
- [17] —, "Spiral-STC: An on-line coverage algorithm of grid environments by a mobile robot," in *2002 IEEE International Conference on Robotics and Automation (ICRA)*, vol. 1, 2002, pp. 954–960.
- [18] M. Theile, H. Bayerlein, R. Nai, D. Gesbert, and M. Caccamo, "UAV Coverage Path Planning under Varying Power Constraints using Deep Reinforcement Learning," in *IEEE/RSJ International Conference on Intelligent Robots and Systems (IROS)*, 2020, pp. 1444–1449.
- [19] P. T. Kyaw, A. Paing, T. T. Thu, R. E. Mohan, A. Vu Le, and P. Veerajagadheswar, "Coverage Path Planning for Decomposition Reconfigurable Grid-Maps Using Deep Reinforcement Learning Based Travelling Salesman Problem," *IEEE Access*, vol. 8, pp. 225 945–225 956, 2020.
- [20] K. G. S. Apuroop, A. V. Le, M. R. Elara, and B. J. Sheu, "Reinforcement Learning-Based Complete Area Coverage Path Planning for a Modified hTrihex Robot," *Sensors*, vol. 21, no. 4, p. 1067, 2021.
- [21] A. Krishna Lakshmanan, R. Elara Mohan, B. Ramalingam, A. Vu Le, P. Veerajagadheswar, K. Tiwari, and M. Ilyas, "Complete coverage path planning using reinforcement learning for Tetromino based cleaning and maintenance robot," *Automation in Construction*, vol. 112, p. 103078, 2020.
- [22] E. M. Arkin, M. A. Bender, E. D. Demaine, S. P. Fekete, J. S. B. Mitchell, and S. Sethia, "Optimal Covering Tours with Turn Costs," *SIAM Journal on Computing*, vol. 35, no. 3, pp. 531–566, 2005.
- [23] I. Vandermeulen, R. Groß, and A. Kolling, "Turn-minimizing multi-robot coverage," in *2019 IEEE International Conference on Robotics and Automation (ICRA)*, 2019, pp. 1014–1020.
- [24] G. L. Nemhauser, *Integer and Combinatorial Optimization*, ser. Wiley-Interscience Series in Discrete Mathematics and Optimization. New York: Wiley, 1999.
- [25] N. Karmarkar, "A new polynomial-time algorithm for linear programming," *Combinatorica*, vol. 4, no. 4, pp. 373–395, 1984.
- [26] L. Pitsoulis, K. Papalamprou, G. Appa, and B. Kotnyek, "On the representability of totally unimodular matrices on bidirected graphs," *Discrete Mathematics*, vol. 309, no. 16, pp. 5024–5042, 2009.
- [27] K. R. Rebman, "Total unimodularity and the transportation problem: A generalization," *Linear Algebra and its Applications*, vol. 8, no. 1, pp. 11–24, 1974.
- [28] A. J. Hoffman and J. B. Kruskal, "Integral Boundary Points of Convex Polyhedra," in *50 Years of Integer Programming 1958-2008: From the Early Years to the State-of-the-Art*. Berlin, Heidelberg: Springer, 2010, pp. 49–76.
- [29] S. L. Smith and F. Imeson, "GLNS: An effective large neighborhood search heuristic for the Generalized Traveling Salesman Problem," *Computers & Operations Research*, vol. 87, pp. 1–19, 2017.
- [30] W. Yang and Y. Wang, "Improved simulated annealing algorithm for GTSP," in *International Conference on Automatic Control and Artificial Intelligence (ACAI)*, 2012, pp. 1202–1205.
- [31] C. Noon and J. Bean, "An Efficient Transformation Of The Generalized Traveling Salesman Problem," *INFOR. Information Systems and Operational Research*, vol. 31, 1993.
- [32] K. J. Obermeyer and Contributors, "VisiLibity: A C++ Library for Visibility Computations in Planar Polygonal Environments," 2008.
- [33] A. O. Makhorin, "GLPK - GNU Project - Free Software Foundation (FSF)," <https://www.gnu.org/software/glpk/>.